Joseph Osumeje et al., J Geol Geophys 2019, 8:1
DOI: 10.4172/2381-8719.1000457

Journal of Geology & Geophysics
ISSN: 2381-8719

Research Article Open Access

# Interpretation of Aeromagnetic and Satellite Data over Part of Maru Schist Belt, Northwestern Nigeria

**Joseph Osumeje O[1]*, Oniku AS[2], Meludu OC[2], Matthew Ogwuche M[1] and Ahmed Usman[3]**

[1]*Department of Physics, Ahmadu Bello University, Zaria, Nigeria*
[2]*Department of Physics, Modibbo Adama University of Technology, Yola, Adamawa state, Nigeria*
[3]*Department of Physics, Kebbi State University, Aliero, Nigeria*

## Abstract

High resolution aeromagnetic data and satellite data covering part the Maru Schist Belt, northwestern Nigeria was interpreted in order to understand the distribution of the surface and the sub-surface magnetic materials within the study area, delineate geologic lineaments and estimate the depth to magnetic sources. Results of the satellite map, the analytic signal and horizontal derivative filters applied on the residual magnetic intensity data reveal that the Maru Schist Belt contains highly magnetic materials suspected to be iron. There is a positive correlation between the lithological map, the satellite map, the aeromagnetic map and the lineament maps. Further analysis of the results shows that iron mineralization (Ferric and Ferrous types) is present in various degrees in the study area. The Euler depth solution has estimated the geological source bodies to be within a depth range of 300–600 m. This is evidence that the Maru Schist Belt was accompanied by series of intense deformation during the orogenic process.

**Keywords:** Analytic signa; Horizontal derivative; Lineaments; Iron; Magnetic source; Maru; Euler depth; Satellite data; Hydrothermal; Alteration; Mineralization

## Introduction

Geophysics involves the application of physical principles and quantitative physical measurements in order to study the earth's interior, its atmosphere and terrestrial space. Of all the geophysical techniques available, the magnetic method is the most widely used [1]. This is due largely to the relative ease and cheapness in acquiring magnetic data. Aeromagnetic data has been used for several purpose such as mineral exploration, oil and gas exploration [2,3], geothermal studies [4-6] and structural delineation [7-10].

Banded Iron Formations (BIF) occur in several localities in Northwestern and central parts of Nigeria [11] and the Maru BIF, located in Zamfara state has been a highly notable zone for different mineralization. Mineral deposits are known to be associated with geologic fractures such as faults and joints. The study area was affected by the Pan-African Orogeny which was accompanied by regional metamorphism, migmatization and extensive granitization and gneissification which produced syntectonic granites and homogeneous gneisses [12].

The interpretation of the aeromagnetic data over part of Maru Schist Belt was done to understand the distribution of magnetic related minerals over the area. The study area is very importance for its great mineralization and the aeromagnetic data interpretation will uncover useful information for further prospecting in the area.

## Location and Geologic Setting of the Study Area

The study area is located around Maru in Zamfara State, Northwestern Nigeria. It is bound by latitudes 12°10' N and 12°30' N, and longitude 6°15' E and 6°30' E as shown in Figure 1. It forms part of the northern Nigerian basement complex which was affected by the Pan-African orogeny. The Maru Schist Belt is considered to be upper Proterozoic supracrustal rocks which have been infolded into the migmatite-gneiss-quartzite complex [13]. Pelitic rocks are dominant within the belt, mainly as phyllites and slates interlaminated with siltstones [12]. Banded iron formation, containing magnetite, hematite and garnet is also present as indicated by the linear (black lines) structure in Figure 1.

## Materials and Methods

High Resolution Aeromagnetic (HRAM) data of Malinchi (Sheet 53), which covers the area under consideration, was obtained from the Nigerian Geologic Survey Agency (NGSA). The data which are in half-degree sheet, were compiled from the data collected at a flight altitude of 80 m, along NE-SW flight lines spaced approximately 500 m apart.

The residual anomaly was separated from the regional magnetic field by using the polynomial fitting method for all the values in the grid. The regional magnetic field contour map of the study area, Figure 2 shows a NE-SW trend in orientation of deeper magnetic sources with an increase in magnetization from NW to SE of the area.

The residual anomaly data was interpolated using a minimum curvature gridding algorithm, available in the Geosoft Oasis Montaj 6.4.2 software, with a grid cell size of 250 m. The resulting residual magnetic anomaly map is presented in Figure 3.

Areas with high magnetic minerals (pink coloured) can be clearly distinguished from areas with low magnetic minerals (blue coloured) in the map (Figure 3). The NNE-SSW trend in high magnetic content is suggestive of the presence of high magnetic minerals within the Maru Schist Belt.

Various filtering techniques were applied on the residual magnetic

***Corresponding author:** Joseph Osumeje O, Department of Physics, Ahmadu Bello University, Zaria, Nigeria, Tel: +2348032919520; E-mail: josumejeh@yahoo.com

**Received** December 18, 2018; **Accepted** January 18, 2019; **Published** January 25, 2019

**Citation:** Osumeje JO, Oniku AS, Meludu OC, Matthew Ogwuche M, Usman A (2019) Interpretation of Aeromagnetic and Satellite Data over Part of Maru Schist Belt, Northwestern Nigeria. J Geol Geophys 8: 457. doi: 10.4172/2381-8719.1000457

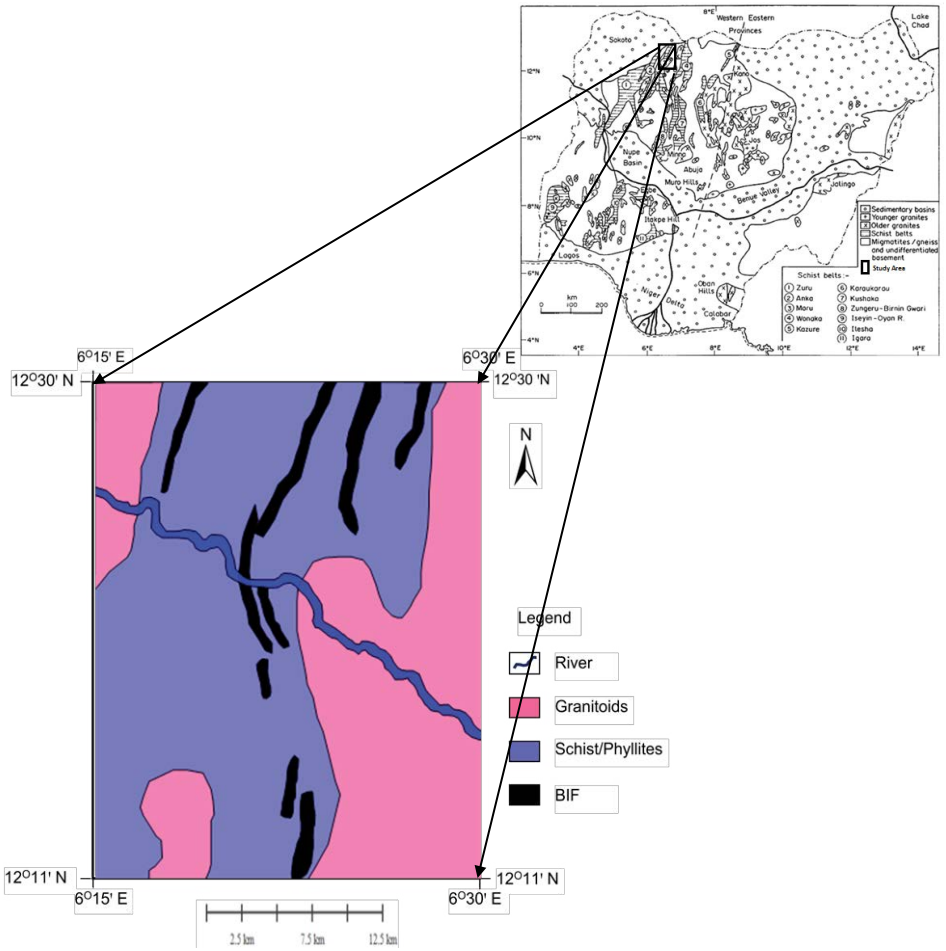


**Figure 1:** Geological Map of part of Maru Schist belt extracted from Kudamnya showing study area and its location.

field grid in order to aid interpretation. These filtering techniques were selected because they best delineate to support the research interest of the work. The techniques include; the analytic signal, the total horizontal derivative and the Euler De convolution techniques. The theories of these techniques are briefly discussed below.

## Analytic signal

The analytic signal technique is based on the use of the first derivative of magnetic anomalies to estimate source characteristics and to locate positions of geologic boundaries such as contacts and faults.

The amplitude of Analytic Signal (AS) is defined as the square root of the squared sum of the vertical and the two horizontal first derivatives of magnetic field anomaly T and is given by [14]:

$$\left|\mathbf{AS}(x,y)\right| = \sqrt{\left(\frac{\partial T}{\partial x}\right)^2 + \left(\frac{\partial T}{\partial y}\right)^2 + \left(\frac{\partial T}{\partial z}\right)^2} \quad (1)$$

One advantage of the Analytic Signal technique is that it defines source positions regardless of any remenant magnetization in the sources [15] hence it's independent of the direction of magnetization. Maxima (ridges and peaks) in the calculated analytic signal of a potential field anomaly map locate the anomalous source body edges and corners.

## Total horizontal derivative

The horizontal gradient method is a simple approach to estimate contact locations of bodies at depths. If T is the magnetic field then the Total Horizontal Derivative (THD) magnitude is given by:

$$\mathrm{THD} = \sqrt{\left(\frac{\partial T}{\partial x}\right)^2 + \left(\frac{\partial T}{\partial y}\right)^2} \quad (2)$$

This function gives a peak anomaly above magnetic contacts under the following assumptions [16]: (i) the regional magnetic field is vertical, (ii) the magnetizations are vertical, (iii) the contacts are vertical, (iv) the contacts are isolated and (v) the sources are thick. Violations of the first four assumptions can lead to shifts of the peaks away from the contacts. Violations of the fifth assumption can lead to secondary peaks parallel to the contacts.

The biggest advantage of the horizontal gradient method is its low sensitivity to the noise in the data because it only requires calculations of the two first-order horizontal derivatives of the field [16].

## Euler De convolution

The Euler De Convolutionis a 3-Dimensional semi-automatic interpretation technique widely used in depth estimation and delimitation of a wide variety of geologic structures. It is based on Euler

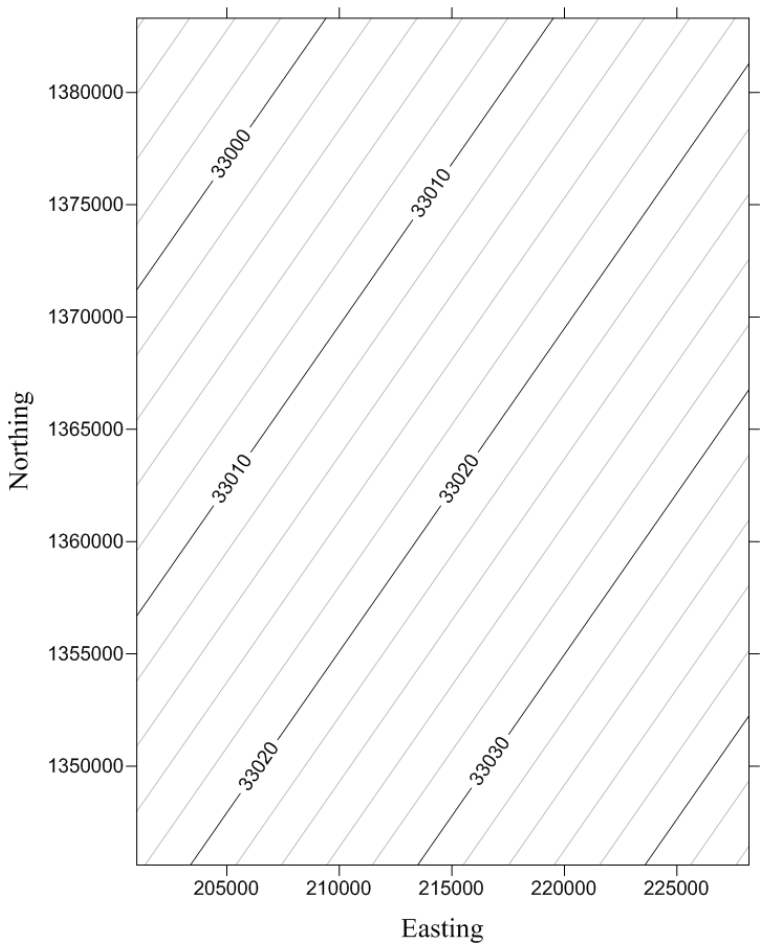


**Figure 2:** Regional magnetic map of the study area.

homogeneity equation (3) which relates the potential field (magnetic or gravity) and its gradient components to the location of the sources, by the degree of homogeneity N, interpreted as a structural index [16].

$$(x - x_o)\frac{\partial T}{\partial x} + (y - y_o)\frac{\partial T}{\partial y} + (z - z_o)\frac{\partial T}{\partial z} = N(B - T) \quad (3)$$

Where T is the total field at (x, y, z) and B is the regional value and N is the structural index. Assuming various measurement point and known N, the above equation can be solved with least squares procedure for unknowns $x_0$, $y_0$, $z_0$ and B.

An important parameter in the Euler equation is the structural index N. This is a homogeneity factor relating the magnetic field and its gradient components to the location of the source. A poor choice of the structural index has been shown to cause a diffuse solution of source locations and serious biases in depth estimation. Both Thompson [17] and Reid [18] suggested that a correct N gives the tightest clustering of the Euler solutions around the geologic structure of interest. Thompson [17] gives more detailed discussion on the degree of homogeneity of potential fields and structural indices of Euler De Convolution.

## Remote sensing technique

A satellite data from the USGS website, the Enhanced Thematic Mapper-Plus (ETM+) data (190/051 path/row, with acquisition date 16 November, 2001) of the Maru area, was obtained for this study. The remote sensing software called ENVI version 4.5 was used to process the data. Since aeromagnetic method respond to variations in magnetic mineralization, and according to Kudamnya [13], Adekoya [11], Obaje [12], the geology of the study area indicates the presence of iron minerals such as ferric and ferrous iron (Megmatite, Heamatite, Goethite, etc). By using the False Colour Composite (FCC) and the band ration techniques, the spatial delineation of the iron mineralization can be obtained. Assigning bands 7, 4, 1 of the ETM+ data to the Red, Green and Blue Channels (RGB) respectively, a FCC image was produced that shows the lithologic mapping of the study area. The Chica-Olma band ratio technique was used to further delineate the iron rich areas in the Ferric and the Ferrous types as shown.

The band ratio (where one band is divided on another band) based on their spectral response was produced using the Mathematical expression below;

$$BV_{i,j,r} = \frac{BV_{i,j,k}}{BV_{i,j,l}} \quad (4)$$

Where; $BV_{i,j,r}$ is the output ratio for the pixel at row i and column j; $BV_{i,j,k}$ is the brightness value at the same location in band k, and $BV_{i,j,l}$ is the brightness value in band l.

With the Chica–Olma ratio technique, a FCC was produced using the band ratios in this order 5/7:5/4:3/1 as Red: Green: Blue respectively to produce the iron mineralization as shown.

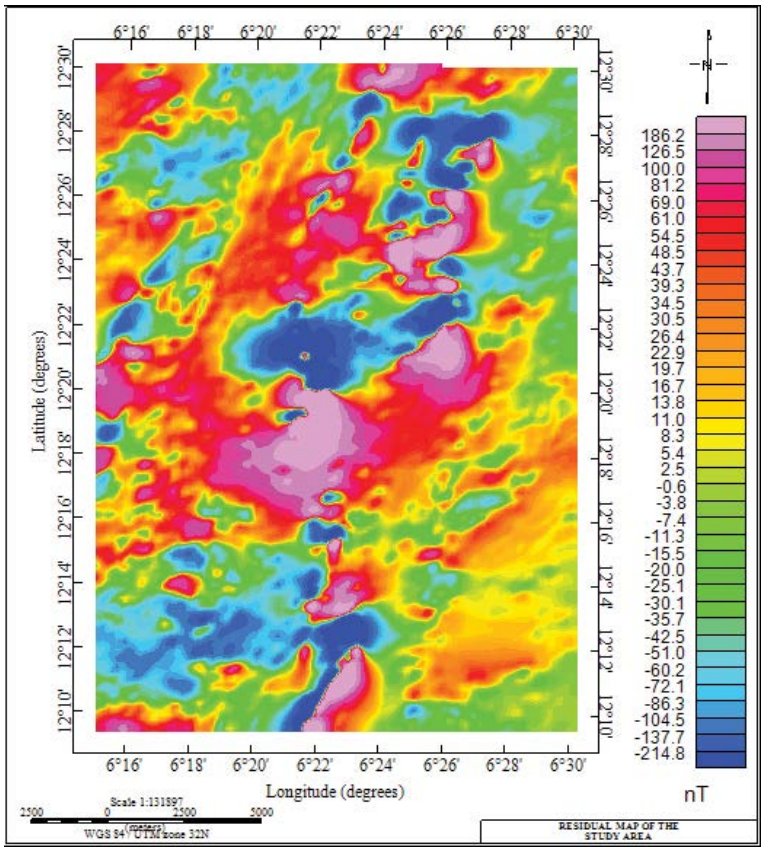


**Figure 3:** Residual magnetic intensity map of the study area.

## Results and Interpretation

### Analytic signal technique

Analytic Signal filtering technique, applied on the residual magnetic field data, is presented in Figure 4. The Analytic Signal (AS) filter helps to detect sources position irrespective of direction and remnant magnetization [14]. It displays maximum amplitude directly over the edge of the magnetic source hence it is used to locate boundaries of magnetic bodies responsible for the anomalies.

On Figure 4, areas with variable magnetic contrast were delineated with the amplitude of analytic signal varying from 0.0122 to 0.9762 nT/m. High amplitude analytic signal values observed can the attributed to the ferrous minerals present in the schist belt. Peak values are observed in villages such as Dan Zara to the south, Zakajiki to the north, Malinchi to the west and Maru in the central part of the study area. Comparing Figure 1 and Figure 4, it can be observed that areas with low AS are underlain mostly by granitoid rocks.

## Total Horizontal Derivative Technique

The anomalies observed on the Total Horizontal Gradient Map (Figure 5) correspond largely to that observed from the analytic signal (Figure 4). The horizontal gradient method provides contact locations that are continuous and thin [7]. The horizontal gradient values ranges from 0.0112 to 0.7744 nT/m and shows a large contrast in magnetic susceptibility along geologic contacts. From Figure 5, magnetic lineaments within the area of study where automatically extracted using the PCI Geomatica 2015 software and the result is shown on Figure 6.

The result (Figure 6) shows the occurrence of several deep source crisscrossing lineaments predominantly trending in the NW-SE direction. This gives further evidence of the extent of deformation that occurred within the belt during the Pan African Orogeny.

### Euler De convolution technique

The Euler De Convolution algorithm was implemented to the gridded residual field intensity map (Figure 3) in order to obtain depth to magnetic sources. Two Structural Indices (SI) were adopted in this work; SI=1 for Dike and Sill models (Figure 7) and SI=2 for Point pole, Line of dipoles and horizontal/vertical cylinder models (Figure 8). This was done in order to obtain well-informed depth information of magnetic materials within the area of study. For both models, a window size of 10 and maximum depth tolerance of 10 % were assumed. From the two maps, the depths to magnetic source within the area are predominantly below 300 m, especially area with suspected faults. However few areas with depths above 600 m are distinguished within the area.

### Remote sensing map

The False Coloured Composite Lithological map is showed in Figure 9. By correlating with Kudamnya [13], the map displays the sandstone as green colour, the granitoids as pink colour, the alluvial deposits as yellow colour and the BIF (metasedimentary) rocks as dark pink colour.

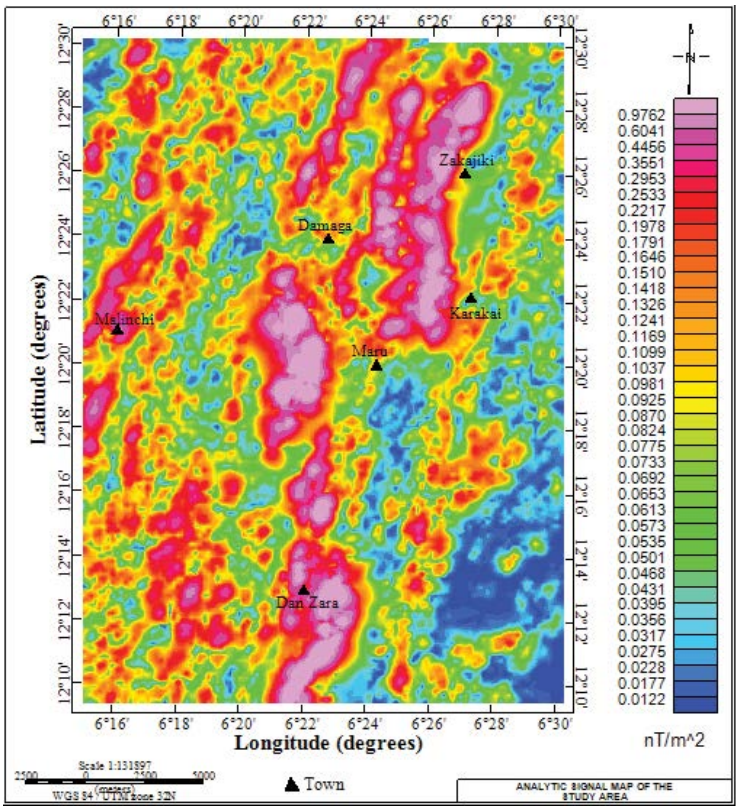


**Figure 4:** Analytic signal map of the study area showing some towns.

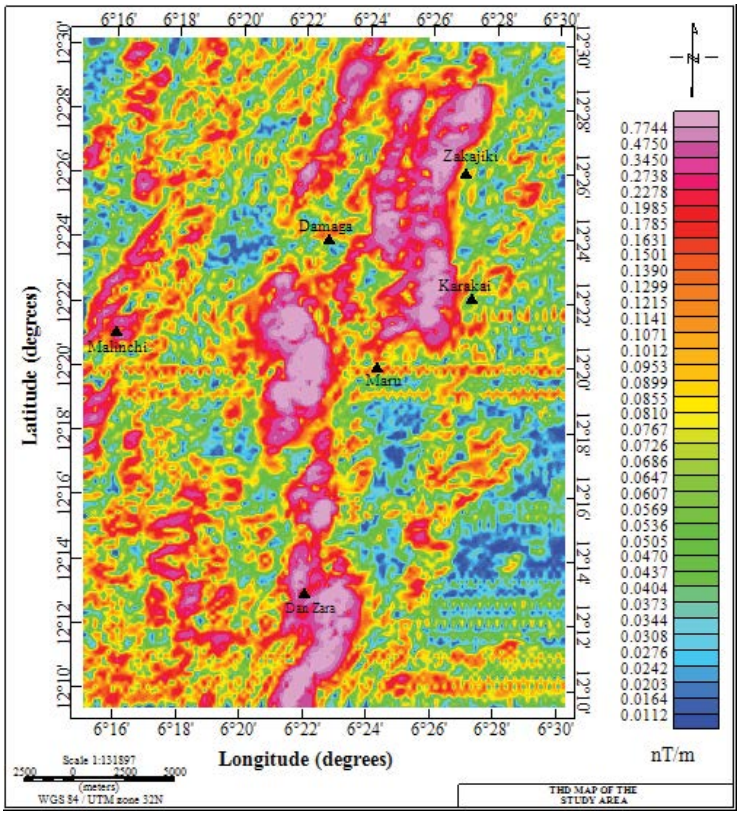


**Figure 5:** Total horizontal derivative map of the study area showing some towns.

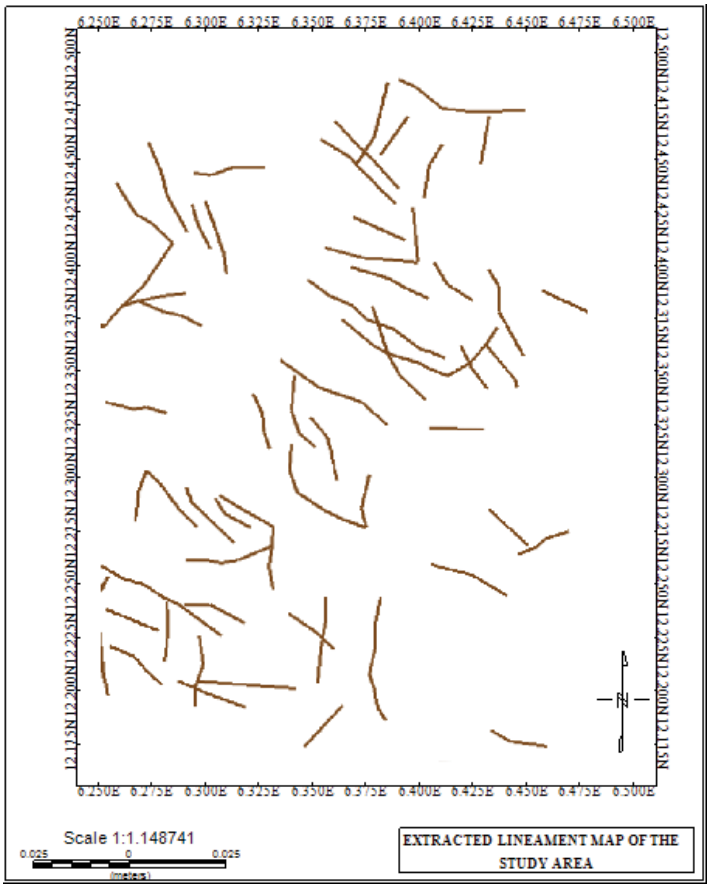


**Figure 6:** Magnetic lineaments within the Maru schist belt.

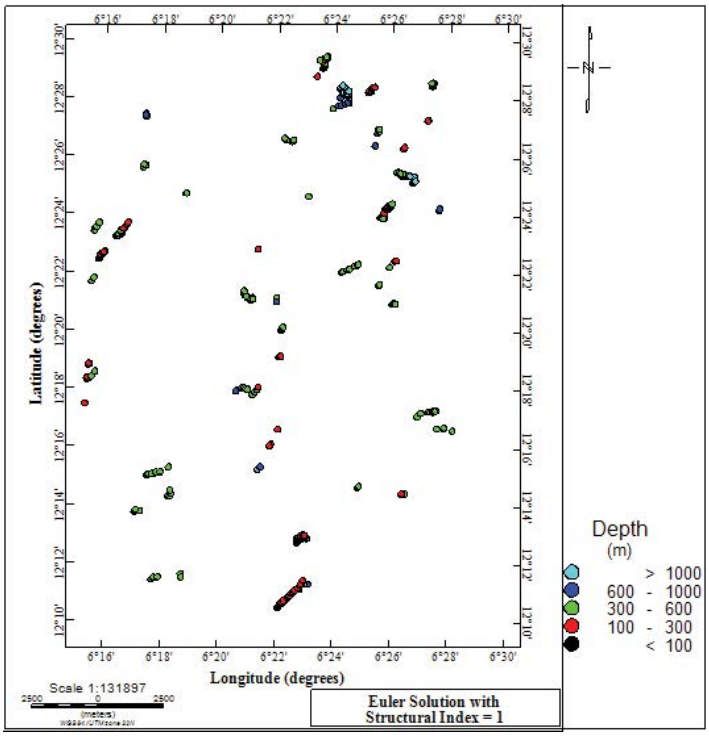


**Figure 7:** Euler depth solution for dike and sill models (Structural Index =1).

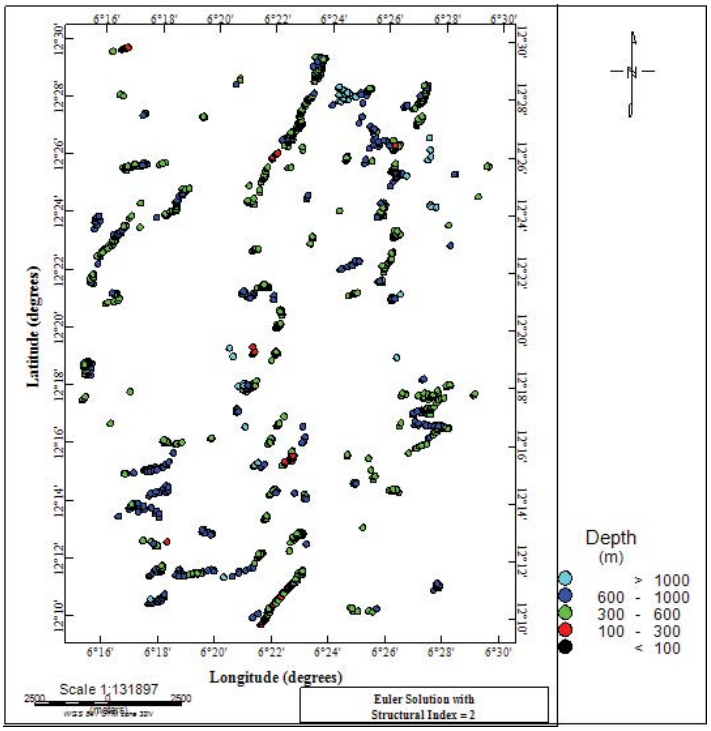


**Figure 8:** Euler depth solution for point pole, line of dipoles and horizontal/vertical cylinder models (Structural Index=2).

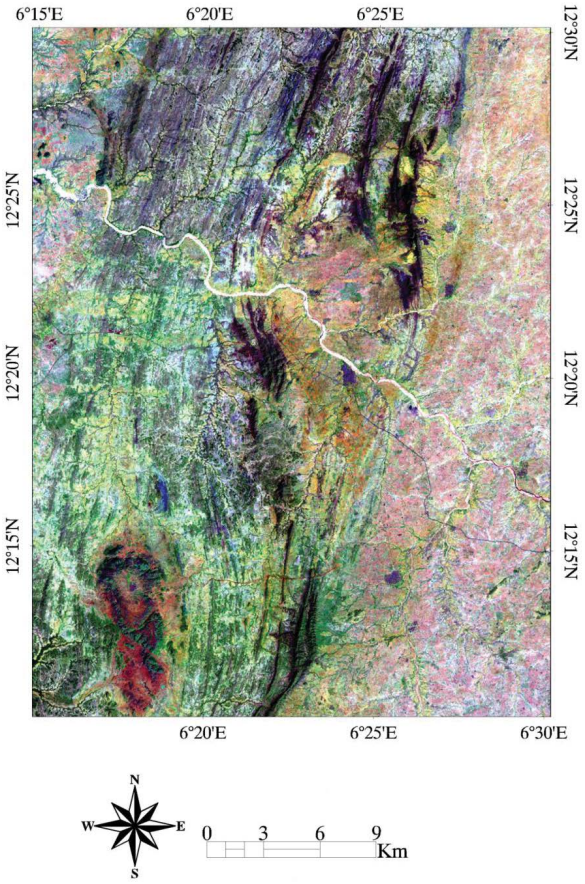


**Figure 9:** Band 7, 4, 1 false colour composite lithological map of the study area.

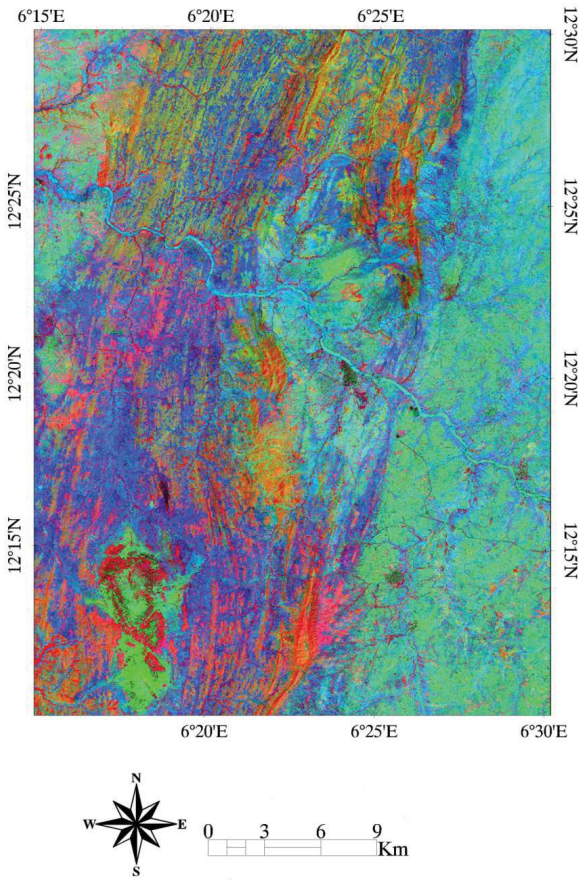


**Figure 10:** Chica-Olma Ratio map for Iron mineralization in the study area.

The Chica-Olma band ratio map in Figure 10 has shown three major colours of red, green and blue. It was observed that band ratio 5/7 displayed the hydrothermally altered clay minerals as light tone, the band ratio 5/4 display the hydrothermally altered ferrous iron minerals as light tones and 3/1 each display the hydrothermally altered ferric iron minerals as light tones. Band ratio 5/7 displayed light tones for clay minerals because the clay minerals have highest reflectance in band 5 and lowest reflectance/absorption in band 7. Similarly, the band ratio 5/4 for the ferrous ($Fe^{2+}$) iron minerals have highest reflectance on band 5 and lowest reflectance on bands 4, and the band ratio 3/1 for the ferric ($Fe^{3+}$) iron minerals have highest reflectance on band 3 and lowest reflectance on bands 1.

It is obvious that the Chica-Olma band ratio (5/7:5/4:3/1), has enhance a hydrothermally altered clay minerals as reddish, hydrothermally altered ferric iron ($Fe^{3+}$) minerals as blue and hydrothermally altered ferrous iron ($Fe^{2+}$) as greenish as shown in Figure 10. Thus, areas within the study area can be distinguished on the basis of their reflectance into the various degrees of clay, of ferric and ferrous iron bearing mineral potentials.

## Discussion

The results have all shown similarities in the structures both on the surface and below the surface of the earth. The iron mineralization map is very much in good correlation with the lithological map and the geological map. Features that supports the existence of iron mineralization has been delineated obviously in all the maps. These maps have also a very positive correlation with the Aeromagnetic Residual Map, the Analytical Signal Map and the Horizontal Derivative Map, where the underground structure are trending in the same directions as the surface exposed structures. Of the two Euler depth solutions, the solution for Point pole, Line of dipoles and horizontal/vertical cylinder models (Structural Index=2) in Figure 8 has shown a positive correlation with the previous maps (Figures 3-6, 9 and 10). The solutions have clustered at places with major fractures or faults.

For the Point pole, Line pole and cylinder (horizontal and vertical) model, the depth to the magnetic (Iron) minerals, with geological structures like Point pole, Line of dipoles and horizontal/vertical cylinder, can be estimated to be between 300–600 m deep with little traces of deeper (between 600 to 1000 m) structures around some of the major fracture or fault locations (Figure 8). For the Dike and the Sill model (Figure 7) with structural index of 1, the depth to the iron mineralization with geological structures of Dikes and Sill is located between 300–600 m deep with a partially distributed shallower depth (between 100–300 m) for such structures.

## Conclusion

The aeromagnetic data and satellite data has been processed and interpreted with some techniques to understand the subsurface geophysical and geological structures of the study area. The Maru Schist Belt, which is a meta sedimentry and sedimentary rock types, is very rich in iron mineralization from the digital aeromagnetic map. The schist belt has shown the presence of hydrothermally

altered iron mineralization (ferric and ferrous) distributed at various degree round the study area. The lineament map has shown a reflection of the lithological map with cluster of lineament around major fault or fractured zones. The Analytical map and the Total horizontal magnetic map correlated positively with the iron mineralization map and the depths to various geological structural model (Dikes, Sills, Point pole, Line pole and cylinder (horizontal and vertical)) have been well established to be between 300-600 m. Structural lineaments predominantly trending NW-SE within the area are also evident. Therefore, the depth to the various magnetic source bodies along major lineaments varies widely in range from 100–1000 m.

## References

1. Moghaddam MM, Sabseparvar M, Mirzaei S, Heydarian N (2015) Interpretation of aeromagnetic data to locate buried faults in north of Zanjan Province, Iran. J Geophys Remote Sensing 4: 143.
2. Chinwuko AI, Onwuemesi AG, Anakwuba EK, Onuba LO, Nwokeabia NC (2012) Interpretation of aeromagnetic anomalies over parts of upper Benue trough and Southern Chad Basin, Nigeria. Adv in App Sci Res 3: 1757-1766.
3. Nwosu OB, Onuba LN (2013) Spectral re-evolution of the magnetic basement depth over part of middle Benue Trough Nigeria using HRAM. Int J Sci Technol Res 2: 97-111.
4. Dolmaz MN, Hisarli ZM, Ustaomer T, Orbay N (2005) Curie point depths based on spectrum analysis of aeromagnetic data, West Anatolian Extensional Province, Turkey. Pure Appl Geophys 162: 571–590.
5. Abraham EM, Lawal KM, AmobiChigozieEkwe AC, Alile O, Murana KA, et al. (2014) Spectral analysis of aeromagnetic data for geothermal energy investigation of Ikogosi Warm Spring-Ekiti State, South-Western, Nigeria. Geothermal Energy 2014 2: 6.
6. Obande GE, Lawal KM, Ahmed LA (2014) Spectral analysis of aeromagnetic data for geothermal investigation of Wikki Warm Spring, north-east Nigeria. Geothermic 50: 85–90.
7. Ndougsa-Mbarga T, Feumoe AN, Manguelle-Dicoum E, Fairhead JD (2012) Aeromagnetic data interpretation to locate buried faults in South-East Cameroon. Geophysica 48: 49–63.
8. Raimi J, Dewu BB, Sule P (2014) An interpretation of structures from aeromagnetic field over a region in Nigerian Younger Granites Province. Int J Geophys 5: 313-323.
9. Graham KM, Kwasi P, Wemegah DD, Boamah D (2014) Geological and structural interpretation of part of the Buem formation, Ghana, Using Aero-geophysical data. J Environ Earth Sci Vol 4.
10. Okpoli CC, Ekere V (2017) Aeromagnetic mapping of the basement architecture of The Ibadan region, South-Western Nigeria. Discovery 53: 614-635.
11. Adekoya JA (1998) The geology and geochemistry of the Maru Banded Iron-Formation, Northwestern Nigeria. J African Earth Sci 27: 241-257.
12. Obaje NG (2009) Geology and mineral resources of Nigeria. Springer.
13. Kudamnya EA, Andongma WT, Osumeje JO (2014) Hydrothermal mapping of Maru Schist Belt, North-Western Nigeria using remote sensing technique. Int J Civil Eng 3: 59-66.
14. Roest WR, Verhoef J, Pilkington M (1992) Magnetic interpretation using 3-D analytic signal. Geophys 57: 116-125.
15. Milligan PR, Gunn PJ (1997) Enhancement and presentation of airborne geophysical data. J Aus Geol Geophys 17: 63-67.
16. Phillips JD (1998) Processing and interpretation of aeromagnetic data for the Santa Cruz Basin-Patahonia Mountains Area, South-Central Arizona. U.S. Geological Survey Open-File Report, Arizona, 2002–98.
17. Thomson DT (1982) EULDPTH: A new technique for making computer-assisted depth estimates from magnetic data. Geophys 47: 31–37.
18. Reid AB, Allsop JM, Granser H, Millet AJ, Somerton IW, et al. (1990) Magnetic Interpretation in three dimensions using Euler De convolution. Geophys 55: 80-91.